농학석사학위논문

# Characterization of glycosylation-related genes in pathogenesis of *Magnaporthe oryzae*

## 벼 도열병균의 병 발생과정에 관여하는 당질화 관련 유전자들의 특성 규명

2013년 8월

서울대학교 대학원

농생명공학부 식물미생물학전공

전 종 범

A THESIS FOR THE DEGREE OF MASTER OF SCIENCE

# Characterization of glycosylation-related genes in pathogenesis of *Magnaporthe oryzae*


**BY**

**Jongbum Jeon**

**Department of Agricultural Biotechnology**

**The Graduate School of Seoul National University**


**August 2013**

농학석사학위논문

# 벼 도열병균의 병 발생과정에 관여하는 당질화 관련 유전자들의 특성 규명

지도교수 이 용 환

이 논문을 농학석사학위논문으로 제출함

2013년 8월

서울대학교 대학원
농생명공학부 식물미생물학전공
전 종 범

전 종 범의 석사학위논문을 인준함
2013년 8월

위 원 장 이 인 원

부위원장 이 용 환

위 원 백 은 우

A THESIS FOR THE DEGREE OF MASTER OF SCIENCE

# Characterization of glycosylation-related genes in pathogenesis of *Magnaporthe oryzae*

UNDER THE DIRECTION OF DR. YONG-HWAN LEE

SUBMITTED TO THE FACULTY OF THE GRADUATE SCHOOL OF SEOUL NATIONAL UNIVERSITY

BY
JONGBUM JEON

MAJOR IN PLANT MICROBIOLOGY
DEPARTMENT OF AGRICULTURAL BIOTECHNOLOGY

AUGUST 2013

APPROVED AS A QUALIFIED THESIS OF JONGBUM JEON
FOR THE DEGREE OF MASTER OF SCIENCE
BY THE COMMITTEE MEMBERS

CHAIRMAN Yong-Won Lee

VICE CHAIRMAN Yong-Hwan Lee

MEMBER Eun Woo Park

# Characterization of glycosylation-related genes in pathogenesis of *Magnaporthe oryzae*

Jongbum Jeon

## ABSTRACT

Rice blast caused by *Magnaporthe oryzae* is one of the most devastating diseases in rice-growing regions worldwide. It is also known as a model system to understand plant-microbe interactions. Proper functioning of the secretory machineries in the ER is important for successful disease development of *M. oryzae*. One of the secretory machineries is glycosylation involved in protein stability and quality control although little is known about roles of glycosylation during disease development by plant pathogenic fungi. Comprehensive BLASTP analysis revealed that 37 homologous genes were identified in *M. oryzae,* based on the glycosylation related genes of *Saccharomyces cerevisiae*. Two of 13 mutants found in the T-DNA mutant library showed defects in pathogenicity. These two mutants have T-DNA insertions near the *MoANP1* and *MoALG8* genes, respectively, and they are

known to play roles in adding glycan during N-glycosylation. To characterize the functions of the genes, additional deletion mutants were generated by a gene replacement strategy. Both Δ*Moanp1* and Δ*Moalg8* mutants showed significantly reduced pathogenicity and invasive growth. The Δ*Moanp1* mutant grew slowly and produced 60% fewer conidia than wild type. The mutant was also susceptible to Congo red, indicating cell wall defects. Also defected to CWDE utility. The Δ*Moalg8* mutant showed no defect in the tested phenotypes compared to wild-type. However, when treated with tunicamycin, an inhibitor of protein glycosylation, expression of six genes involved in the UPR pathway was strongly up-regulated. Similarly, the genes were also up-regulated in the Δ*Moalg8* mutant without the treatment of tunicamycin. Taken together, this study provides the evidence that N-glycosylation is important in the pathogenicity of *M. oryzae*.

**KEYWORDS**: Glycosylation, *Magnaporthe oryzae*, pathogencity, secretory pathway

Student number: 2011-23535

# CONTENTS

# LIST OF TABLES

# LIST OF FIGURES

# INTRODUCTION

The plant pathogenic fungus, *Magnaporthe oryzae* is the pathogen of rice blast and pathogenic to around 50 monocotyledonous crops (Couch *et al.*, 2005). It is one of the most devastating plant-pathogenic fungi in the world, seriously affecting rice yield (Talbot, 2003). *M. oryzae* is a hemibiotrophic fungus converting its lifestyle during the infection process. These two nutrient-trophisms are divided into early biotrophic phase during the initial host infection stage and later necrotrophic phase where acquisition of the nutrient occurs in the dead host cell (Ebbole, 2007). The fungus is a causal agent of model system for studying plant-pathogen interactions. As the fungus has been extensively studied, to genomic approach and molecular biological techniques are available (Dean *et al.*, 2005; Ebbole, 2007; Valent, 1990).

The disease cycle of fungus is composed of several developmental steps. Conidia from the fungus are dispersed by wind or raindrop and land on the surface of host by chance. The adhered conidia germinate in humid condition and form a dome-shaped structure called appressorium at the end of germ tubes. In the melanized appressoria, accumulation of the solutes such as glycerol generates the turgor pressure of 8 MPa required before the penetration of host cell wall (Howard *et al.*, 1991). During the penetration, the fungus mechanically makes bleaches on the plant surface, and then produces the

infectious structure, penetration peg, to enter the plant cell. This structure develops to the primary hyphae. Subsequently, bulbous invasive hypha encroach the infected cell and invade the adjacent cells (Kankanala *et al.*, 2007). After colonizing the plant cells, invasive hypha generate conidia for secondary inoculum to carry on the second disease cycle (Ou, 1985). Especially in the early stage of invasive step, primary hyphae makes up the specific structure called the biotrophic interfacial complex (BIC). This structure is known to act as a secretion structure where effectors are secreted into plant cells. (Khang *et al.*, 2010; Mosquera *et al.*, 2009)

Most host-pathogen interactions are complicated systems, and poorly understood about them. When the host and pathogens interact together, the host is struggled to avoid pathogenic infection and operate defense mechanisms in response against pathogens (Stukenbrock and McDonald, 2009; van de Veerdonk *et al.*, 2008). Among this system, secretion of effectors is also included (Rafiqi *et al.*, 2012).

Many proteins are secreted by specific machinery. The secretion systems are mainly classified into classical secretory pathway and non-classical pathway (Bendtsen *et al.*, 2004). In the classical secretory pathway, proteins trail through the specific organelle path. Firstly, the secreted proteins with signal peptide are translocated to the interior of endoplasmic reticulum. After translocation, proteins are shipped to the extracellular space via intracellular

organelles through Golgi apparatus and vesicles (Lippincott-Schwartz *et al.*, 2000). In pathogenic fungi, secreted proteins work various biological activities such as cell wall component production in developmental stages (Chaffin *et al.*, 1998), signal transmission (Mauri and Bosma, 2012), and interactions with the host (Stergiopoulos and de Wit, 2009). Many of secreted proteins, translocated to outer cellular space has been studied. However machineries involved in the secretion process are poorly understood. Recently, a P-type ATPase (APT2) (Gilbert *et al.*, 2006), Molecular chaperone (LHS1) (Yi *et al.*, 2009), Snare protein (SEC22) (Song *et al.*, 2010) are identified in *M. oryzae* and they are essential for the process of several secreted proteins related to pathogenic process. But only a few genes encoding protein related to secretory machinery identified.

Glycosylation is an important step with many secretory machineries. It is processed by attachment of a glycan on asparagine residue of specific site either the N-X-S/T motif, glycosylated site of N-glycosylation (Bause, 1983) or one of the sites at hydroxyproline, hydroxylysine, threonine and serine, glycosylated site of O-glycosylation (Carraway and Hull, 1989). After adding the glycan on the specific site, glycan structure is further branched by glycosylation related genes. For the cellular part, glycosylation of proteins plays the important roles in protein stability, secretion and localization (Deshpande *et al.*, 2008; Lee *et al.*, 2003). Glycoproteins suspended on

membrane mediate the cell to cell communication by using the glycan components (Crocker and Feizi, 1996). The both groups of N and O-glycosylation are well identified in *S. cerevisiae* among the other fungal species group (Herscovics, 1999; Lussier *et al.*, 1997). Only a few mechanisms are known about glycosylation in filamentous fungus, mainly particular genera including *Aspergillus* spp. and *Trichoderma* spp. (Maras *et al.*, 1999). The secretion machinery, glycosylate most plant cell wall degrading enzymes (plant CWDE) (Annis and Goodwin, 1997) and check the quality of the secreted proteins used the unfolded protein response (UPR) pathway (Branza-Nichita *et al.*, 2000). In spite of glycosylation related genes are well studied in other fungal species, none of those was identified in *M. oryzae*.

In this study, two novel glycosylation genes related to pathogenicity were identified. The disruption of *MoANP1* showed defects on invasive growth, vegetative growth and conidiation. Especially mutant was vulnerable to cell wall stress. *MoALG8* affected invasive growth and UPR pathway respectively. In consequence, the result will be one of clues for deciphering the function of glycosylation in pathogenesis.

# MATERIALS AND METHODS

## I. Bioinformatical analysis

To identify the homologous of glycosylation related genes in *Magnaporthe oryzae*, the reference genes were firstly gathered from *Saccaromycetes cerevisiae* by using BLASTP algorithms serviced at the Comparative Fungal Genomics Platform 2.0 (CFGP) (Choi *et al.*, 2012). The loci of genes were co-predicted by percentage of homology and Inparanoid 7 available at the Inparanoid project site ((Ostlund *et al.*, 2010); http://inparanoid.cgb.ki.se/).

## II. Fungal strains and culture condition

*M. oryzae* strain KJ201 conserved as a stock in the Center for Fungal Genetic Resources (CFGR) was used as the wild type. Gene deletion mutants were manufactured by the KJ201 background and were cultured in oatmeal agar media (5% oatmeal (w/v), 2.5% agar powder (w/v)) or V8 agar media (8% V8 juice (v/v), 1.5% agar powder (w/v)) at 25℃ under the constant light condition.

## III. T-DNA insertion mutant confirmation and pathogenicity screening

To identify the locus insertion affected, inverse PCR was performed and conidia were harvested from V8 juice agar media at 5 dpi and 2 days of

aeration. It was performed by spraying conidial suspension ($5x10^4$ conidia/mL), containing 250 ppm Tween 20 on 3 weeks old Nakdongbyeo. Inoculated rice plants were incubated for 18 hours in a dew chamber (dark, 100% humidity, 27℃) and transferred to a light chamber (27℃). Pathogenicity was estimated after 6 days by pathogenicity index (Valent *et al.*, 1991).

**IV. Targeted deletion of *MoALG8, MoANP1* genes and complementation**

Protoplasts were generated from mycelia of KJ201, grown in liquid complete media (1% saccharose (w/v), 0.6% yeast extract (w/v), 0.6% casamino acid (w/v)) for 5 days. The mycelia compartment were harvested and treated with 0.3% lysing enzyme. Harvested, protoplasts were diluted with 1x STC (20% sucrose (w/v), 50 mM Tris-HCl, 50 mM $CaCl_2$). Gene replacement was progressed by homologous recombination systems. Knock-out constructs were fused by three step double joint PCR (Yu *et al.*, 2004). 5' and 3' flanking of target genes were amplified by PCR and jointed with *HPH* cassette amplified from pBCATPH (Yun, 1998). Full construct injected to KJ201 protoplast by PEG mediated transformation. Transforms were selected on TB3 agar media (0.3% yeast extract (w/v), 0.3% casamino acid (w/v), 1% glucose (w/v), 20% sucrose (w/v), 0.8% agar powder (w/v)) containing 200 ppm hygromycin B. Gene deletion mutants were screened by Southern

analysis. Genomic DNA of transformants was extracted by NucleoSpin® Plant II DNA extraction kit (Macherey-Nagel, Dfren, Germany). After restriction enzyme digestion, the fragments of product were slowly separated by agarose gel electrophoresis. DNA in the gel was transferred to nitrocellulose membrane, Hybond-N+ (GE healthcare, NJ, USA) and hybridized with radioisotope labeled probes. Probes were made by Rediprime™ II Random Prime Labeling System kit (GE healthcare, NJ, USA). Hybridized nitro cellulose membrane exposed to imaging plate, BAS-2040 (Fuji Photo Film, Tokyo, Japan) and scanned by phosphorimage analyzer, BAS-1000 (Fuji Photo Film, Tokyo, Japan).

**V. Developmental phenotype assay**

Vegetative growth was measured by radial size of mycelia on modified complete media (1% glucose (w/v), 0.2% peptone (w/v), 0.1% yeast extract (w/v), 0.1% casamino acid (w/v), 0.1% trace element (v/v), 0.6% sodium nitrate (w/v), 0.05% potassium chloride (w/v), 0.05% magnesium sulfate (w/v), 0.15% potassium dihydrogen phosphate (w/v), 1.5% agar powder (w/v)) (Talbot *et al.*, 1993) at 9 days from inoculation. Conidiation measuring counted the number of conidia, grown on V8 juice agar media at 5 dpi and 2 days of aeration. Conidia were harvested with 5 mL of sterilized distilled water and counted using hemacytometer. Conidiophore development was monitored

cross sections of scraped piece from colony grown on oatmeal agar (Lau and Hamer, 1998). Conidial germination and appressoria formation were measured by counting the variety of conidia dropped on cover slip by conidial suspension ($2x10^4$ conidia /mL). This was measured at 16 hours in moistened box. Pathogenicity was experimented by spraying conidial suspension ($5x10^4$ conidia/mL) on leaves of 3~4 weeks aged Nakdongbyeo. Inoculated rice was incubated for 12 hours in dew chamber (100% humidity, 27℃, dark condition) and moved to chamber which modulated the light circumstance cycled 18 hour light and 6 hour dark condition (27℃). Pathogenicity was estimated 7 days after spaying.

**VI. Expression analysis by quantitative real-time PCR**

For quantitative real-time PCR, total RNA extraction of background samples were cultured from conidial suspension in complete liquid media for 2 days and treated with two chemicals, 10 ㎍/㎖ DTT (Disulfide bond inhibitor) in 60 minutes and 10 mM Tunicamycin (N-glycosylation inhibitor) in 30 minutes. TRIZOL reagent and easy-spin™ Total RNA Extraction Kit (iNtRON Biotechnology, Seongnam, Korea) were used to extract the total RNA from each sample. After that, cDNA was synthesized by Superscript First-strand Synthesis System III (Invitrogen Life Technologies, CA, USA)

with 5 $\mu g$ of Total RNA. Quantitative real-time PCR was experimented as previously described (Kim *et al.*, 2005) with 7500 Real-Time PCR system (Applied Biosystems, CA, USA). For the detection of relative expression, SYBR GREEN PCR Master Mix (Applied Biosystems, CA, USA) was used and Primer pairs listed in Table 1 were used. Reaction was performed for 3 min of denaturation at 95°C, the 40 cycles of reaction were performed by this conditions: 15s at 95°C, 30s at 60°C, and 30s at 72°C. Quantitative RT-PCR was performed twice with three experimental repeats, and all of data are presented.

**VII. Cell Wall integrity and utilization of plant CWDE**

Cell wall integrity was measured by medial growth on complete agar media with cell wall stress agents, 0.01% Sodium dodecyl sulfate, 200 ppm congo red and 200 ppm calcofluor white was used for assay. The inoculums are sectioned into the mycelial disc grown at minimal agar media (MMA) (1% glucose (w/v), 0.1% trace element (v/v), 0.6% sodium nitrate (w/v), 0.05% potassium chloride (w/v), 0.05% magnesium sulfate (w/v), 0.15% potassium dihydrogen phosphate (w/v), 1.5% agar powder (w/v)), 7 days. Cell wall integrity was measured by relative radial growth in cell wall stress medium at 9 days after inoculation. Utilization of plant cell wall degrading enzymes was

also measured by radial growth on mono-carbon source contained media. Each of conditions is based on the carbon starvation media (same components as MMA except absence of glucose). Except the C starvation media contained the 1% glucose (MMA), 1% cellobiose, 1% xylan and 1% xylose. It was measured by relative radial growth compared to wild-type tendency at 9 dpi.

**VIII. Infection assay**

Detached sheath of shoot at 5~6 leaves aged (Zadoks scale 13~14) (Zadoks *et al.*, 1974). Nakdongbyeo were used for sheath inoculation assay. Conidial suspension of $4x10^4$ conidia / mL prepared and injected into detached sheath of rice. Inoculated leaves were incubated in constitutive humidity container at 25℃ and observed at 48 hpi. The observed samples were sliced from sheath by razor blade and observed with optical microscope. It was observed the 100 penetration points for calculating the portion of invasive patterns.

## Table 1. Primers used in this study

| Primer name | Sequence (5'→3') |
|---|---|
| *For confirmation of T-DNA insertion mutants:* | |
| RB3 | CCCTTCCCAACAGTTGCGCA |
| RB1n_R | GTTTTCCCAGTCACGACGTTGTAA |
| *For generation and confirmation of knockout mutants:* | |
| *HPH*_F | GGCTTGGCTGGAGCTAGTGGAGG |
| *HPH*_R | CTCCGGAGCTGACATCGACACCAAC |
| MGG_05686T0 5'F | CCCAAGTTGCGGTATGCGTAG |
| MGG_05686T0 5'R | CCTCCACTAGCTCCAGCCAAGCCAATAGTGGGGACAGCAAATTCCA |
| MGG_05686T0 3'F | GTTGGTGTCGATGTCAGCTCCGGACGGTGTGTAAATTGGACCAATTGT |
| MGG_05686T0 3'R | GTGCAGAAAGGCGTGGTCG |
| MGG_06191T0 5'F | CGCGCCACACTTGACCTTC |
| MGG_06191T0 5'R | CCTCCACTAGCTCCAGCCAAGCCCGGCCTATCAAATTGATTAAAATTTG |
| MGG_06191T0 3'F | GTTGGTGTCGATGTCAGCTCCGGATCCAAGCAGTCTCGTCGTAGGA |
| MGG_06191T0 3'R | GATCAAGCCGTTGGAGTGGG |
| *For confirmation of knockout mutants:* | |
| MGG_06191T0_qRT_F | ATATGACGGTGAATGAGCAGG |
| MGG_06191T0_qRT_R | CTTGATAGGGTTGAGGTCGTG |
| MGG_05686T0_qRT_F | TTACCAGTTCTTACACGGCAG |
| MGG_05686T0_qRT_R | TCCCTTTACCATCAAGACGC |
| *For confirmation of UPR pathway:* | |
| MoLHS1_qRT_F | ACCCAGTCCTTACCATCAAG |
| MoLHS1_qRT_R | CTATCTTAACCGGCTTGTCC |
| MoKAR2_qRT_F | AACGGTCTCGAGAACTATGC |
| MoKAR2_qRT_R | TCCTTCTGCTCCTCAAAATC |
| MoSIL1_qRT_F | GACTTAGAGGGTCTGCCTGT |
| MoSIL1_qRT_R | GAAGTACATGTCGTGGGAAA |
| MoSCJ1_qRT_F | GGTCACGTAGAGATGGTCAA |
| MoSCJ1_qRT_R | CCTGTATTTCTCCCACACTG |
| MoPDI1_qRT_F | GTTGTCGCTTACTTGTCCAG |

| | |
|---|---|
| MoPDI1_qRT_R | CGTCAAATTTCTTGTCGAAG |
| MoIRE1_qRT_F | ATGATTGAGAAGGTGCGGAG |
| MoIRE1_qRT_R | AGAGCGGATTGGTGAAAAGAG |
| Beta-TUB_qRT_F | ACAACTTCGTCTTCGGTCAG |
| Beta-TUB_qRT_R | CTCCAGGGTTTCCAGATCAC |

*MoLHS1* (MGG_06648T0), *MoKAR2* (MGG_02503T0), *MoSIL1* (MGG_10843T0), *MoSCJ1* (MGG_07502T0), *MoPDI1* (MGG_05753T0), *MoIRE1* (MGG_01067T0), *Beta-TUB* (β-tubulin, MGG_00604T0).

*HPH* marker was amplified from pBCATPH vector.

# RESULTS

## I. Selected genes encoding putative glycosylation protein in *M. oryzae*

Searching for the putative glycosylation homologs of *M. oryzae*, the reference glycosylation gene based on the *S. cerevisiae* genome was gathered (Deshpande *et al.*, 2008; Geysens *et al.*, 2009). Previously, 54 yeast genes were studied for glycosylation. From that 37 genes were selected by using BLASTP and Inparanoid 7. These genes are counterpart of yeast homologs (Table 1). The First step towards detecting the homology of proteins between *S. cerevisiae* and *M. oryzae* genome was BLASTP performed with glycosylation set of proteins against the reference genome. There were 35 genes having over 30% of similarity towards the orthologs of *S. cerevisiae*. The unmatched 8 genes were excluded and additional 10 genes were collected by Inparanoid 7 which was used to avoid the outparalogs of corresponding genes of two species (O'Brien *et al.*, 2005).

## II. Selection of T-DNA insertion mutants related to glycosylation involved in pathogenesis in *M. oryzae*

A total of 7 genes (Table 2) encoding putative glycosylation proteins were selected from computational process and through ATMT database, they were

named from their orthologs of *S. cerevisiae*. The 7 mutants confirmed to have T-DNA insertion within 1.5kb upstream and 0.5kb downstream from the ORF (Figure 1). They were all confirmed to have an insertion site and T-DNA copy numbers by inverse PCR analysis (Ochman *et al.*, 1988) and southern blot analysis. The screened 7 mutants had only one copy of T-DNA correctly inserted within boundary. Among the 7 mutants, mutation on 2 genes showed a defect on pathogenicity (Figure 2). *MoANP1* and *MoALG8* encoding putative glycosylation proteins were decreased in index compared to WT. These names came from their counterpart of yeast genes *Scanp1* and *Scalg8*. This project is focused on the two of the eight genes related to pathogenesis characterized yet. (Table 3).

**III. Targeted replacement of *MoANP1* and *MoALG8* genes**

Gene deletion mutants were manufactured by targeted gene replacement with a resistance marker cassette. It was used by homologous recombination and knockout constructs double jointed with up and downstream 1.2 kb~1.5 kb of each genes and *HPH* cassette. Protoplasts were transformed with these constructs. Gene deletion was confirmed by Southern blot analysis and RT-PCR of transcript (Figure 3).

**Table 2. List of glycosylation genes background by *in silico* analysis**

| | Saccharomycetes cerevisiae | | Magnaporthe Oryzae | | | |
|---|---|---|---|---|---|---|
| [a]Synthesis of ER-precursor structure for N-glycosylation | Gene name | Locus | Locus | [b]BLASTP | | [c]Inparanoid |
| UDP-N-acetyl-glucosamine-1-P transferase | ALG7 | YBR243C | MGG_01559T0 | 49.11% | 1.00e-117 | |
| N-Acetylglucosaminyldiphosphodolichol N-acetylglucosaminyltransferase: catalytic part | ALG13 | YGL047W | MGG_07272T0 | 30.49% | 6.00e-12 | Unmatched |
| N-Acetylglucosaminyldiphosphodolichol N-acetylglucosaminyltransferase: transmembrane part | ALG14 | YBR070C | MGG_17724T0 | 37.83% | 4.00e-07 | |
| Chitobiosyldiphosphodolichol b-mannosyltransferase | ALG1 | YBR110W | MGG_10494T0 | 34.44% | 6.00e-62 | |
| Glycolipid 3,6-a-mannosyltransferase activity | ALG2 | YGL065C | MGG_02384T0 | 44.94% | 2.00e-88 | |
| GDP-mannose:Man(3/4)GlcNAc(2) a-1,2-mannosyltransferase | ALG11 | YNL048W | MGG_03883T0 | 39.94% | 5.00e-77 | |
| Flippase | RFT1 | YBL020W | MGG_08271T0 | 31.86% | 2.00e-62 | |
| Dol-P-mannose:Man(5)GlcNAc(2)-PP-dolichyl a-1,3-mannosyltransferase | ALG3 | YBL082C | MGG_08010T0 | 36.31% | 8.00e-66 | |
| Dol-P-mannose:Man(6/8)GlcNAc(2)-PP-dolichyl a-1,2-mannosyltransferase | ALG9 | YNL219C | MGG_14835T0 | 33.27% | 6.00e-79 | |
| Dol-P-mannose:Man(7)GlcNAc(2)-PP-dolichyl a-1,6-mannosyltransferase | ALG12 | YNR030W | MGG_09909T0 | 31.76% | 8.00e-60 | |
| Dol-P-glucose:Man(9)GlcNAc(2)-PP-dolichyl a-1,3-glucosyltransferase | ALG6 | YOR002W | MGG_09310T0 | 40.10% | 1.00e-110 | |
| Dol-P-glucose:Glc(1)Man(9)GlcNAc(2)-PP-dolichyl a-1,3-glucosyltransferase | ALG8 | YOR067C | MGG_05686T0 | 45.47% | 1.00e-119 | |
| Dol-P-glucose:Glc(2)Man(9)GlcNAc(2)-PP-dolichyl a-1,2-glucosyltransferase | ALG10s | YGR227W | MGG_03990T0 | 23.68% | 8.00e-35 | Matched |
| Dolichyl-phosphate b-D-mannosyltransferase (polypeptide 1) | DPM1 | YPR183W | MGG_16862T0 | 34.59% | 2.00e-25 | |
| Dolichyl-phosphate glucosyltransferase | ALG5 | YPL227C | MGG_06137T0 | 37.82% | 2.00e-64 | |

| | | | | | | |
|---|---|---|---|---|---|---|
| The oligosaccharyl transferase (OST) | | | | | | |
| Alpha subunit (essential) of OST—ribosphorin I | OST1 | YJL002C | MGG_09287T0 | 29.81% | 6.00e-50 | Matched |
| Epsilon (essential) subunit of OST | OST2 | YOR103C | MGG_05758T0 | 45.11 % | 4.00e-21 | Matched |
| Essential subunit of OST | STT3 | YGL022W | MGG_04773T0 | 60.40% | 0 | |
| Beta (essential) subunit of OST | WBP1 | YEL002C | MGG_02821T0 | 29.61% | 6.00e-47 | Matched |
| Delta (essential) subunit of OST—Ribophorin II | SWP1 | YMR149W | MGG_03687T0 | 22.34% | 9.00e-10 | Matched |
| Gamma subunit of OST | OST3 | YOR085W | MGG_04500T0 | 26.26% | 8.00e-19 | Matched |
| Subunit of OST | OST4 | YDL232W | | | | |
| Zeta subunit of OST | OST5 | YGL226C-A | | | | |
| Subunit of OST | OST6 | YML019W | | | | |
| ER-processing of N-glycans and protein quality control | | | | | | |
| Glucosidase I | CWH41 | YGL027C | MGG_04045T0 | 36.99% | 1.00e-150 | |
| Glucosidase II—alpha subunit | ROT2 | YBR229C | MGG_08623T0 | 37.72% | 0 | |
| → Other glycosyl hydrolase family 31 members | | | | | | |
| Glucosidase II—beta subunit | GTB1 | YDR221W | MGG_16417T0 | 28.72% | 1.00e-20 | Matched |
| ER degradation enhancer, a-1,2-mannosidase-like protein (EDEM) | MNL1 | YHR204W | MGG_00667T0 | 36.24% | 8.00e-98 | |
| ER-mannosidase I (and Man9-mannosidase) → other glycosyl hydrolase family 47 members | MNT1 | YDR483W | MGG_08692T0 | 43.36% | 1.00e-110 | |
| ER-mannosidase II | (AMS1 | YGL156W | MGG_04464T0 | 45.43% | 0 | Unmatched |
| | | | MGG_12735T0 | 33.90% | 0 | Unmatched |
| ER quality control lectin belonging to the OS-9 protein family | YOS9 | YDR057W | MGG_02297T0 | 24.76% | 2.00e-13 | Unmatched |

| | | | | | | |
|---|---|---|---|---|---|---|
| Golgi processing of N-glycans | | | | | | |
| Initiating a-1,6-mannosyltransferase | OCH1 | YGL038C | MGG_02859T0 | 33.83% | 2.00e-60 | Unmatched |
| Subunit of Golgi mannosyltransferase complexes M-Pol I and M-Pol II | MNN9 | YPL050C | MGG_00171T0 | 47.71% | 2.00e-92 | |
| Subunit of Golgi mannosyltransferase complex M-Pol I | VAN1 | YML115C | MGG_12335T0 | 54.16% | 1.00e-107 | Unmatched |
| Subunit of Golgi mannosyltransferase complex M-Pol II | ANP1 | YEL036C | MGG_06191T0 | 46.92% | 3.00e-78 | |
| Subunit of Golgi mannosyltransferase complex M-Pol II | MNN10 | YDR245W | MGG_00164T0 | 54.96% | 4.00e-95 | |
| Subunit of Golgi mannosyltransferase complex M-Pol II | MNN11 | YJL183W | MGG_15865T0 | 28.23% | 6.00e-25 | Matched |
| Subunit of Golgi mannosyltransferase complex M-Pol II | HOC1 | YJR075W | MGG_02859T0 | 41.66% | 1.00e-62 | |
| | | | MGG_03361T0 | 30.07% | 4.00e-25 | Unmatched |
| Golgi a-1,2-mannosyltransferase | MNN2 | YBR015C | MGG_07729T0 | 33.33% | 1.00e-37 | |
| Golgi a-1,2-mannosyltransferase | MNN5 | YJL186W | MGG_02268T0 | 29.15% | 2.00e-34 | Matched |
| Putative positive regulator of the mannosylphosphate transferase | MNN4 | YKL201C | MGG_05727T0 | 41.21% | 1.00e-30 | Unmatched |
| N-Acetylglucosaminyltransferase | GNT1 | YOR320C | | | | |
| Synthesis of Structure for O-glycosylation | | | | | | |
| Protein O-mannosyltransferase gene family | PMT1 | YDL095W | MGG_02954T0 | 43.65% | 1.00e-175 | |
| Protein O-mannosyltransferase gene family | PMT2 | YAL023C | MGG_07190T0 | 48.33% | 0 | |
| Protein O-mannosyltransferase gene family | PMT3 | YOR321W | | | | |
| Protein O-mannosyltransferase gene family | PMT4 | YJR143C | MGG_04427T0 | 46.92% | 0 | |
| Protein O-mannosyltransferase gene family | PMT5 | YDL093W | | | | |
| Protein O-mannosyltransferase gene family | PMT6 | YGR199W | | | | |
| alpha-1,2-Mnt-encoding genes | MNT1 | YDR483W | | | | |

| | | | | | | |
|---|---|---|---|---|---|---|
| alpha-1,2-Mnt-encoding genes | KTR1 | YOR099W | MGG_08692T0 | 63.35% | 1.00e-132 | |
| alpha-1,2-Mnt-encoding genes | KTR2 | YKR061W | | | | |
| alpha-1,3-Mnt-encoding genes | MNN1 | YER001W | | | | |
| alpha-1,3-Mnt-encoding genes | MNT2 | YGL257C | | | | |
| alpha-1,3-Mnt-encoding genes | MNT3 | YIL014W | MGG_09806T0 | 26.68% | 1.00e-18 | Matched |

[a] Categorized by *S. cerevisiae* genes already identified the function of genes

[b] BLASTP were performed by CFGP. Measure the numeric identity and e-value as *S. cerevisiae* S288C genome to M. oryzae ver. 8 genome

[c] Inparanoid 7.0 was operated by local system. The result shown the differently collected gene are notified and the others not notified are same as “Matched”

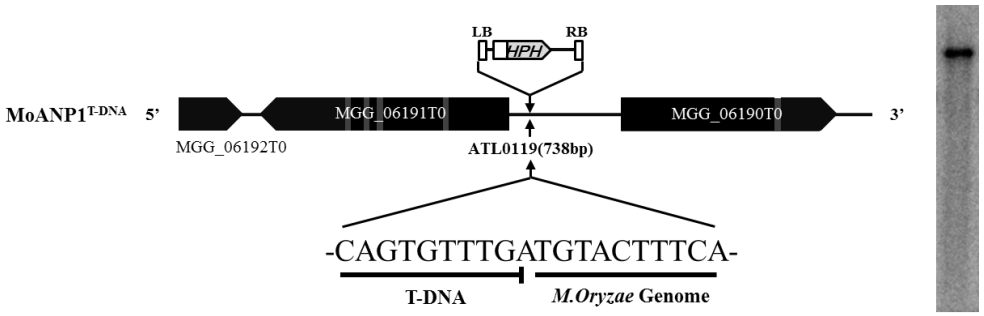
LB
RB
HPH
MoANP1T-DNA
5'
MGG_06191T0
MGG_06190T0
3'
MGG_06192T0
ATL0119(738bp)
-CAGTGTTTGATGTACTTTCA-
T-DNA
M.Oryzae Genome

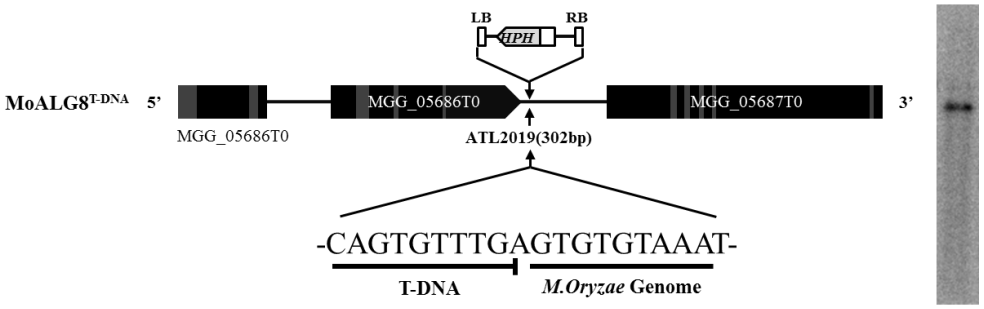
LB
RB
HPH
MoALG8T-DNA
5'
MGG_05686T0
MGG_05687T0
3'
MGG_05686T0
ATL2019(302bp)
-CAGTGTTTGAGTGTGTAAAT-
T-DNA
M.Oryzae Genome

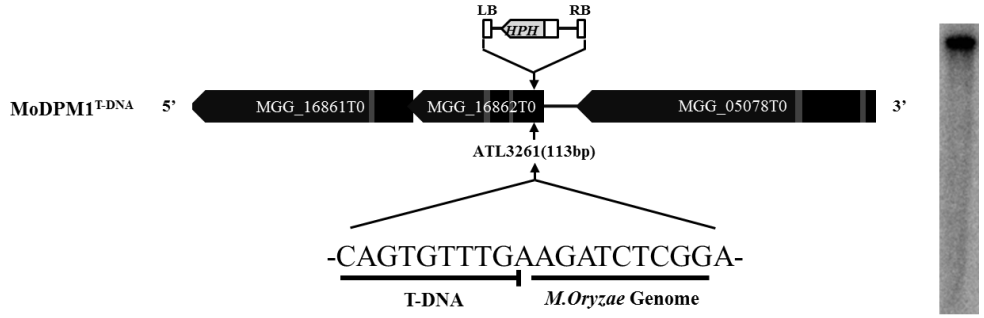
LB
RB
HPH
MoDPM1T-DNA
5'
MGG_16861T0
MGG_16862T0
MGG_05078T0
3'
ATL3261(113bp)
-CAGTGTTTGAAGATCTCGGA-
T-DNA
M.Oryzae Genome

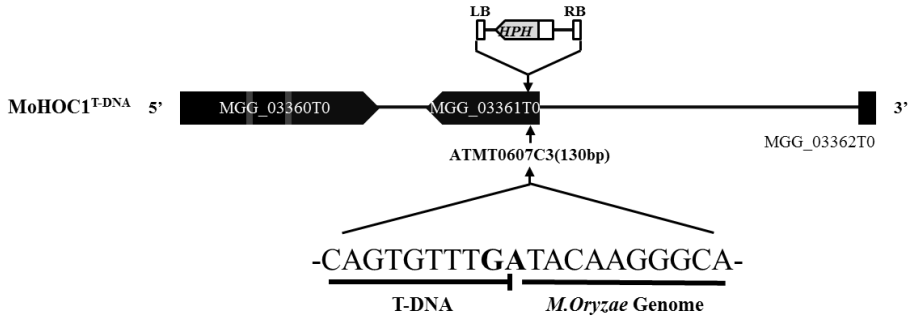
LB
RB
HPH
MoHOC1T-DNA
5'
MGG_03360T0
MGG_03361T0
3'
MGG_03362T0
ATMT0607C3(130bp)
-CAGTGTTTGATACAAGGGCA-
T-DNA
M.Oryzae Genome

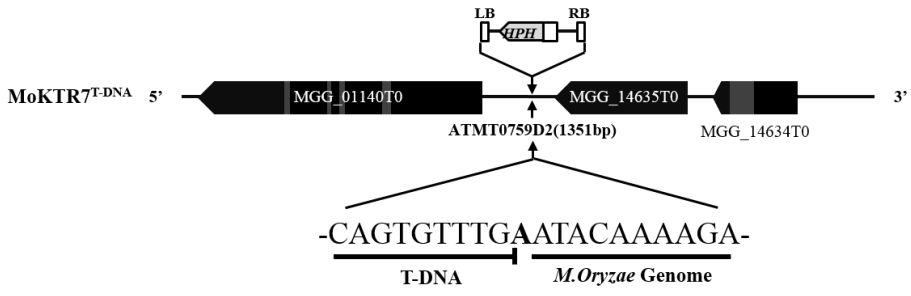
LB
RB
HPH
MoKTR7T-DNA
5'
MGG_01140T0
MGG_14635T0
3'
ATMT0759D2(1351bp)
MGG_14634T0
-CAGTGTTTGAATACAAAAGA-
T-DNA
M.Oryzae Genome

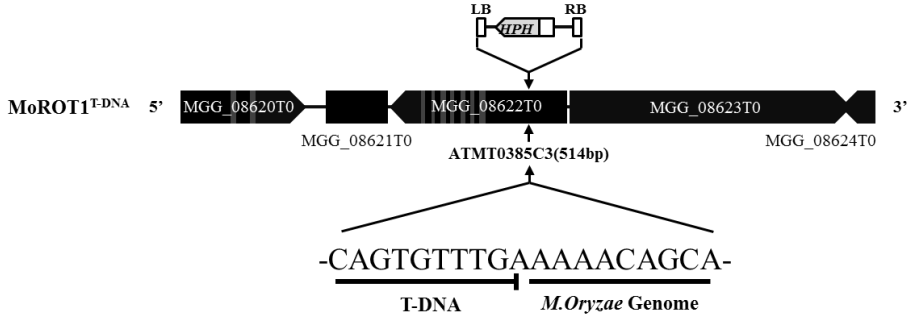
LB
RB
HPH
MoROT1T-DNA
5'
MGG_08620T0
MGG_08622T0
MGG_08623T0
3'
MGG_08621T0
MGG_08624T0
ATMT0385C3(514bp)
-CAGTGTTTGAAAAACAGCA-
T-DNA
M.Oryzae Genome

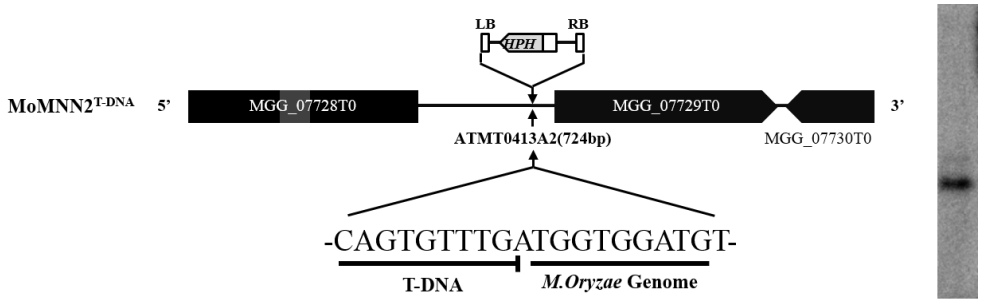


**Figure 1. Confirmation of T-DNA insertion**

Schematic diagrams of T-DNA insertion in listed mutants. To confirm the T-DNA insertion site, Genomic DNA of each mutants were prepared and inverse PCR was performed left part of each figure shown the result of insertion site from loci. The numeric in parenthesis beside the name of T-DNA insertion mutants is notifying the distance from ORF of targeted locus. The right part of the figure shows the result of southern hybridization with each mutant. Genomic DNA was fully digested with *Hind*III and hybridized with *HPH* fragment as a probe.

**Table 3. List of glycosylation genes related T-DNA insertion mutants**

| Gene name[a] | *M. oryzae* loci | T-DNA insertion mutants | Insertion site[b] |
|---|---|---|---|
| *MoANP1* | MGG_06191T0 | ATL0119 | 738bp of 5’ |
| *MoALG8* | MGG_05686T0 | ATL2019 | 302bp of 3’ |
| *MoDPM1* | MGG_16862T0 | ATL3261 | 113bp of 5’ |
| *MoHOC2* | MGG_03361T0 | ATMT0607C3 | 130bp of 5’ |
| *MoROT1* | MGG_08622T0 | ATMT0385C3 | 514bp of 5’ |
| *MoKTR7* | MGG_14635T0 | ATMT0759D2 | 1350bp of 5’ |
| *MoMNN2* | MGG_07729T0 | ATMT0413A2 | 724bp of 5’ |

[a] T-DNA Insertion mutants named from orthologs of *S. cerevisiae.*

[b] T-DNA inserted site from end of open reading frame region.

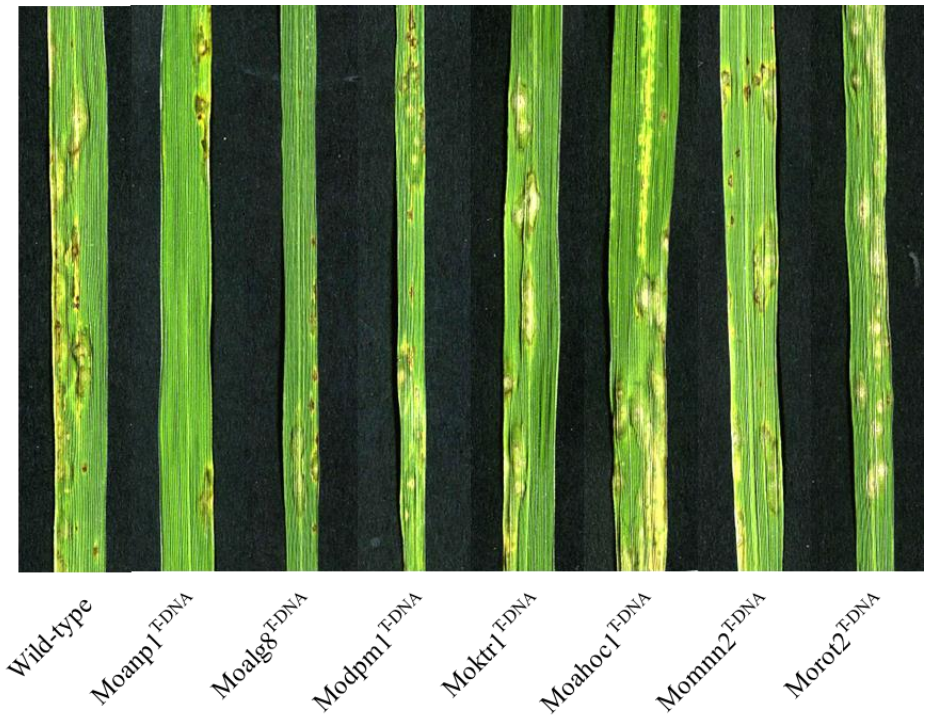


**Figure 2. Pathogenicity of T-DNA insertion mutants related on glycosylation**

In order to measure the pathogenicity, conidial suspension ($5x10^4$ conidia / mL) of each transformant was collected from V8 agar media. Conidial suspension was sprayed to 3-4 weeks aged rice leaves and lesions of disease were observed at 7 dpi.

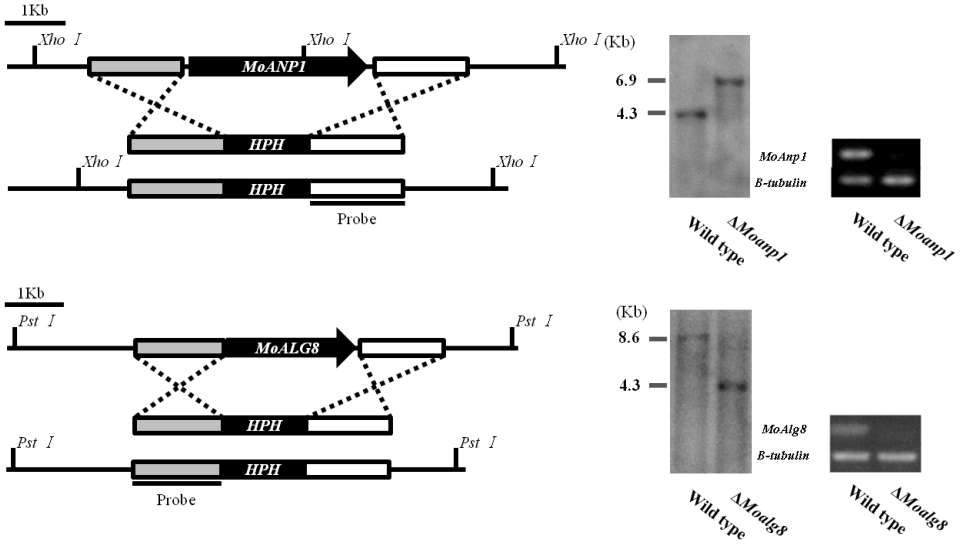


**Figure 3. Generation of gene deletion mutants**

Sticks indicate the ORF of two genes and the flanking regions and *HPH* cassette drown by boxes. To confirm the knockout mutants, Southern analysis and Reverse Transcriptase PCR were performed. Bands with expected sizes demonstrate the correct deletion of the target genes by homologous recombination. Absent of band in figure of RT-PCR double confirm the target gene deletion.

**IV. Developmental phenotypes and pathogenicity of Δ*Moanp1*, Δ*Moalg8* mutants**

The inspection of developmental phenotypes in vegetative growth, conidiation, conidial germination, appressoria formation were performed to decipher the pathogenic effects by gene deletion. During vegetative growth, Δ*Moanp1* showed a significant growth defect (36.5 mm) compared with wild-type growth (53.2 mm) at 9 dpi. The complementation mutants recovered the radial growth compared to gene deletion mutants (Figure 5) Conidia development was observed by optical microscope 24 hour after induction of colony disc from OMA. Δ*Moanp1* produced a few conidiophores on the mycelia (Figure 6A) and Δ*Moanp1* produced 40% of conidia compared with number of conidia in wild-type. The conidia production was significantly decreased. The reduced condiation was recovered in the complemented mutant (Figure 6B). Thus Δ*Moanp1* affects the conidiation. Although the Δ*Moalg8* did not show any defects before the penetration, there was no visible defect in conidial germination and appressoria formation (Table 4).

Pathogenicity tests were performed to determine the importance of glycosylation involving the two genes during infection. Conidial suspension was sprayed on 3-4 week aged leaves of Nakdongbyeo cultivar. Nakdongbyeo does not have any known R genes, making it a susceptible cultivar to all strains.

Therefore, Pathogenicity of KO mutants inoculated on this cultivar reveal the function of respective deletion genes. Pathogenicity was compared with the wild-type at 7dpi. Both Δ*Moanp1* and Δ*Moalg8* showed a reduction of pathogenicity. Each complemented mutant restored virulence, producing larger lesions than respective gene deletion mutants (Figure 4). These evidences imply the *MoANP1* and *MoALG8* are related to pathogenesis of *M. oryzae*.

**Table 4. Developmental phenotypes of transformants including T-DNA mutants, gene deletion mutant and complements**

| Strain | Mycelial growth[a] (mm) | Conidiation[b] ($10^4$/mL) | Germination[c] (%) | Appressoria formation[d] (%) |
|---|---|---|---|---|
| Wild-type | 55.5±0.9 | 17.9±1.3 | 99.0±1.0 | 97.5±0.9 |
| Moalg8$^{T\text{-}DNA}$ | 55.3±0.8 | 17.1±0.9 | 99.3±0.2 | 98.4±2.0 |
| Δ*Moalg8* | 57.2±0.8 | 18.8±0.4 | 99.7±0.6 | 96.8±0.6 |
| *Moalg8c* | 56.5±0.9 | 16.7±0.7 | 97.3±1.6 | 98.1±1.6 |
| *Moanp1*$^{T\text{-}DNA}$ | 57.7±0.6 | 15.3±1.2* | 95.9±2.2 | 98.7±0.5 |
| Δ*Moanp1* | 39.0±1.7* | 10.6±0.4* | 97.7±2.1 | 99.8±0.3 |
| *Moanp1c* | 48.3±0.6 | 17.1±1.3 | 95.9±1.3 | 97.7±0.6 |

[a] Diameter of radial growth on complete media were measured at 9 dpi.

[b] Conidia were harvested on V8 agar media at 5 dpi and 2 days aeration, the number of conidia was counted.

[c] The percentage of germinated conidia on hydrophobic surface was counted the numeric at 16 hpi in the humid condition.

[d] The percentage of appressoria formation counted by rate of conidia which have formed appressorium by conidia which had been germinated conidia on hydrophobic surface at 16 hpi in the humid condition.

* Data which observed significant difference compared to the wild type were marked on asterisk. Statistical analysis used the Tukey method.

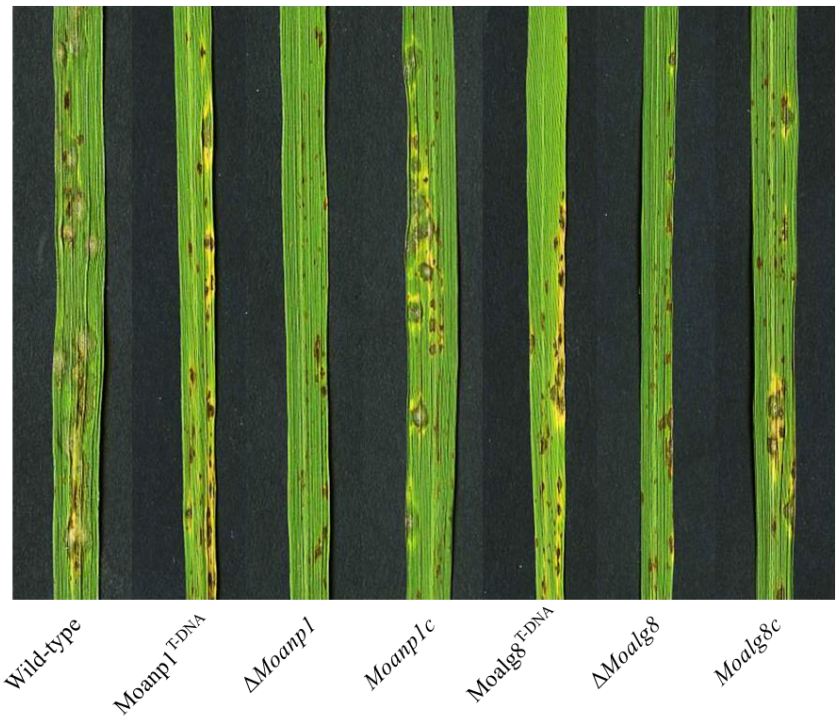


**Figure 4. Effect of Δ*Moanp1* and Δ*Moalg8* genes on pathogenicity**

In order to measure the pathogenicity, conidial suspension ($5x10^4$ conidia / mL) of each strain was collected from V8 agar media. Conidial suspension was sprayed to 3-4 weeks aged rice leaves and lesions of disease were observed at 7 dpi.

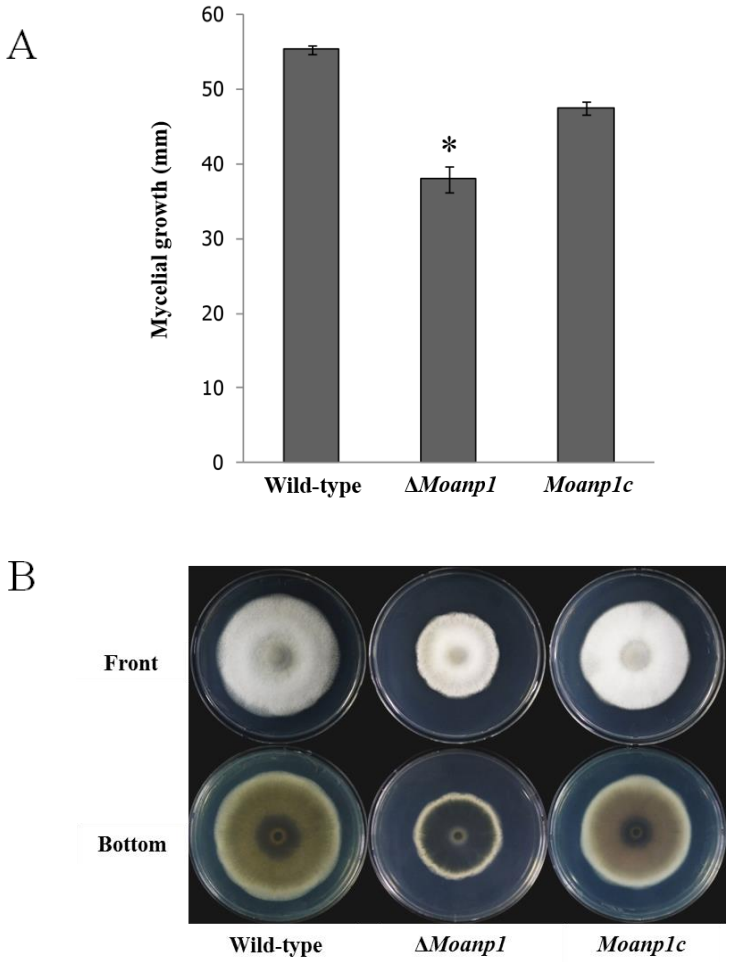


**Figure 5. Vegetative growth defect of Δ*Moanp1***

(A) Mycelial growth is measured by its diameter of colony inoculated 9 days * Data which observed significant difference compared to the wild type were marked on asterisk. Statistical analysis used the Tukey method.

(B) Colony morphology on CM agar media inoculated from block of colony on MM agar media. Photograph were taken at 9 days after inoculation

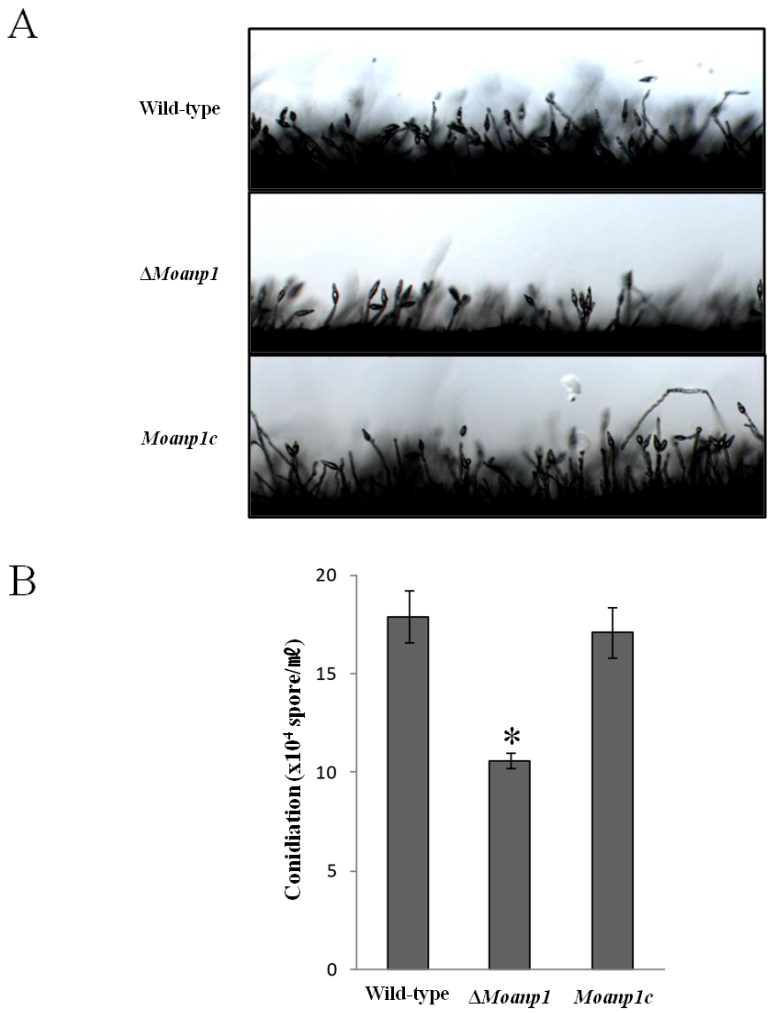


**Figure 6. Conidiation defect of Δ*Moanp1***

(A) Conidia development was observed by optical microscope 24 hour after induction of colony disc from OMA

(B) Count the number of conidia incubated from V8 media 5 days and aerated 2 days

* Data which observed significant difference compared to the wild type were marked on asterisk. Statistical analysis used the Tukey method.

**V. Retardation of invasive growth**

In order to decipher the reduced pathogenesis, invasive growth in rice sheath was performed. To test whether the reduction of pathogenicity in Δ*Moanp1* and Δ*Moalg8* were due to defect on the invasive growth, two mutants were grown on the rice sheath. In the result, Δ*Moanp1* showed the retardation of invasive growth at 48 hpi (Figure 7A). Most of invasive hyphae of Δ*Moalg8* were captured in primary infected cell (Figure 8A). To quantify the invasive hyphal pattern, a hundred infection points were observed. In the wild type, most of invasive hyphae were invasion to multiple cells were observed that 75% of infection point in wild-type. While Δ*Moanp1* showed the multiple cell invasion which were counted only 20% (Figure 7B). Furthermore Δ*Moalg8* were observed 10% of infection point invade the multiple cells compared to 70% of point captured in one cell (Figure 8B). In these result, Δ*Moanp1* was decreased the invasive growth and Δ*Moalg8* affects invasive growth.

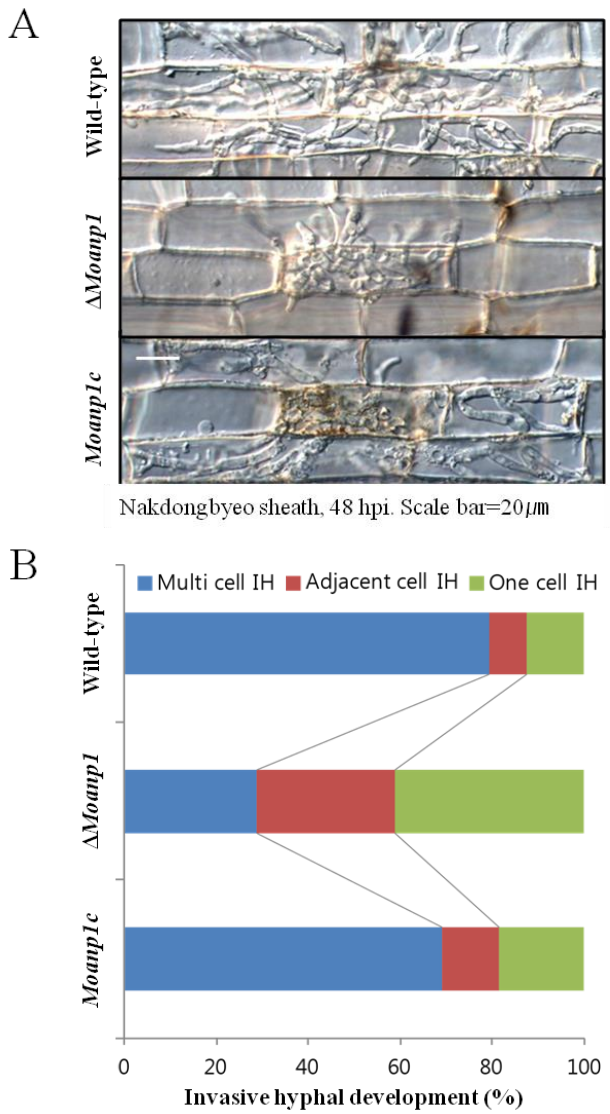


**Figure 7. Invasive growth of Δ*Moanp1 in planta***

(A) Conidial suspension inoculated in rice sheath. White bar indicates the size of 20um. Invasive growth was observed at 48 hpi.

(B) Quantification of pattern of invasive growth. Over 100 infection points were classified

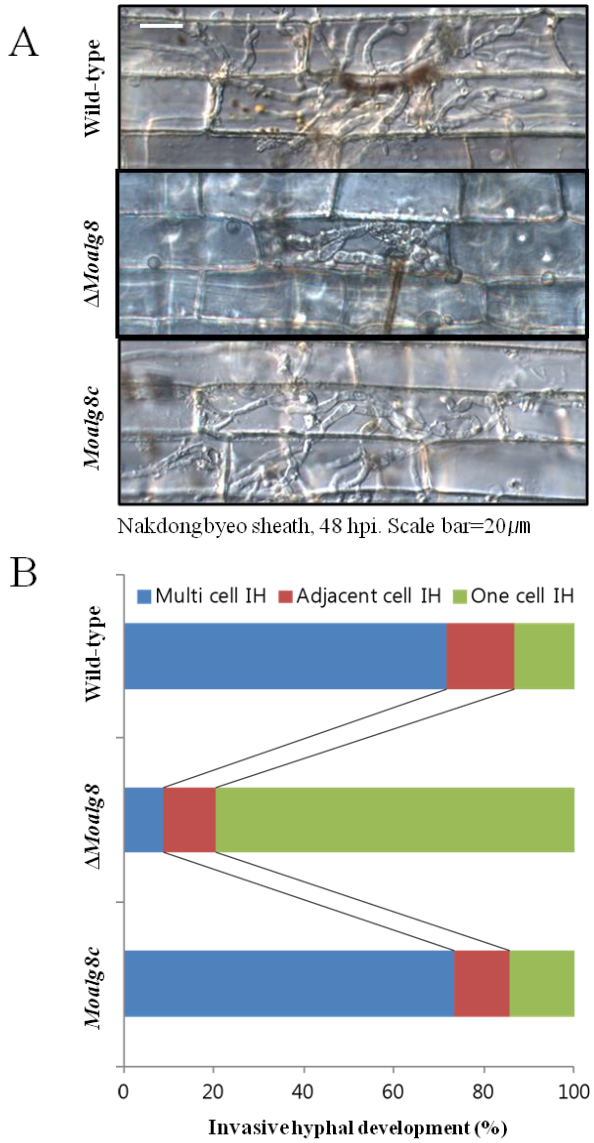


**Figure 8. Invasive growth of Δ*Moalg8 in planta***

(A) Conidial suspension inoculated in rice sheath. White bar indicates the size of 20um. Invasive growth was observed at 48 hpi.

(B) Quantification of pattern of invasive growth. Over 100 infection points were classified

**VI. Retarded vegetative growth of Δ*Moanp1* in other conditions**

To compare the difference of growth retardation for several other conditions, measured relative growth rate compared to respective wild-type radial growth length. Because growth of Δ*Moanp1* in complete media has been shown. The relative growth rate was normalized by the radial growth on the complete media. To determine the cell wall integrity of Δ*Moanp1*, vegetative growth in cell wall stress medium was observed. Among the CM agar with 0.01% SDS, 200 ppm congo red (CR) and 200 ppm calcofluor white (CFW), relative growth retardation was significantly decreased in CFW(55%) and CR(68%) added media. These decrease was recovered in complement mutants (119% and 78%), but growth of SDS condition (90%) was not significant different to that of complete media (79%) (Figure 9). Thus, Δ*Moanp1* is concluded as vulnerable to cell wall stress.

Furthermore, to determine plant cell wall degradation enzymes (CWDE) activity, vegetative growth in mono-carbon source medium was observed. These mono-carbon sources were composed of cellobiose, dimer of cellulose and xylan, component of hemi-cellulose. Each growth pattern of components was compared to the positive control (MMA) and negative control (C starvation media). The growth retardation was observed in cellobiose source condition (66%) and xylan source condition (70%). This pattern was similar

to C starvation growth (73%), but significantly different to that of Minimal media condition (81%) and complement mutants of three significantly conditions were also recouped the growth pattern of wild-type (Figure 10). Thus, Δ*Moanp1* affected the activities of plant CWDE.

**VII. *MoALG8* induced by ER stress, and Genes of UPR pathway are regulated by target gene disruption.**

UPR pathway is one of the key early secretion mechanisms in cells. When proteins are secreted, misfolded proteins are extradited to UPR pathway for degradation (Hampton, 2000). To characterize whether expression of target genes and other related genes occur at various conditions including stress conditions and gene disruption conditions, quantitative RT-PCR was performed using the RNA extracted from those conditions. When ER stress was induced by treatment of stress agent, 10mM DTT 30 and 10 ㎍/㎖ tunicamycin, expression of genes are regulated by that conditions. These two agents have shown the induction of genes, associated with post-translation modification in filamentous fungi and *M. oryzae* (Kasuya *et al.*, 1999; Yi *et al.*, 2009). These genes are homologs of Scj1p (an Hsp40 family protein), Sil1p 9 a nucleotide exchange factor), Pdip1 (protein disulfide isomerase) and Ire1p (transmembrane Ser/Thr kinase and endoribonuclease), which are

related to UPR pathway of *S. cerevisiae*. Also *MoLHS1* and *MoKAR2* are included in these genes. (Yi *et al.*, 2009) Upon DTT or tunicamycin treatment, the expression of these 6 genes was induced more than two-fold compared to that of beta-tubulin (Figure 11A). Similarly in the transcript level of gene disruption conditions, these 6 genes were induced more than two-fold (Figure 11B).

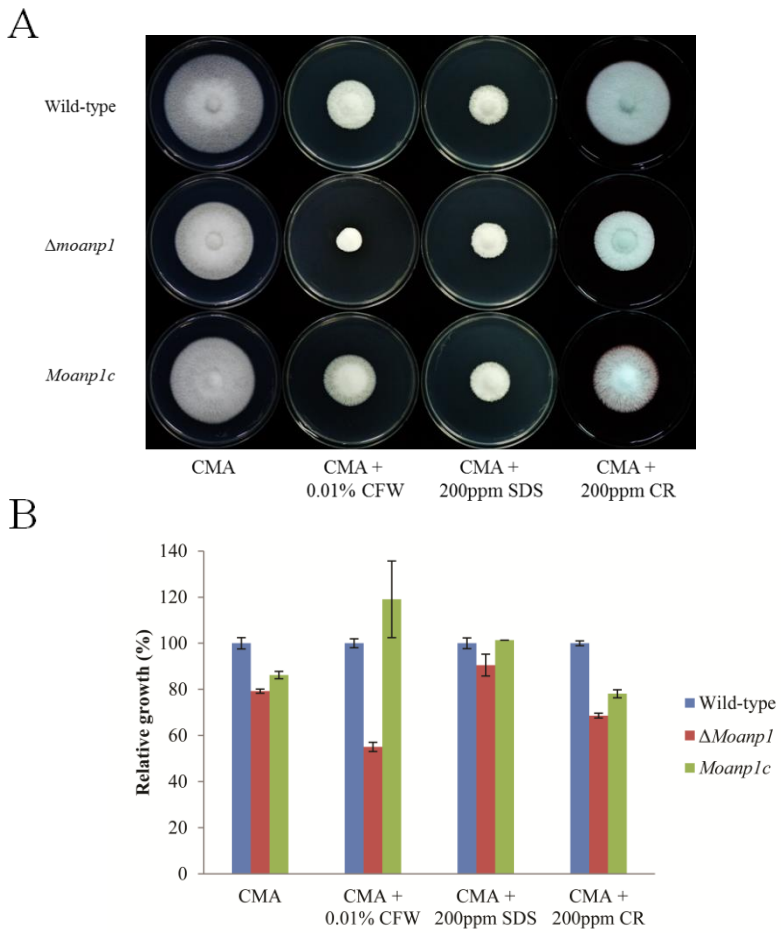


**Figure 9. Cell wall disruption of Δ*Moanp1***

Mycelia disc were inoculated on cell wall stress agent containing complete media (CMA). Growth was measured at 9 dpi. Three added agents are calcoflour white (CFW), sodium dodecyl sulfate (SDS) and congo red (CR). (A) Photograph was taken on the 9 days from inoculation. (B) Growth was measured by relative growth late compared to growth of wild-type.

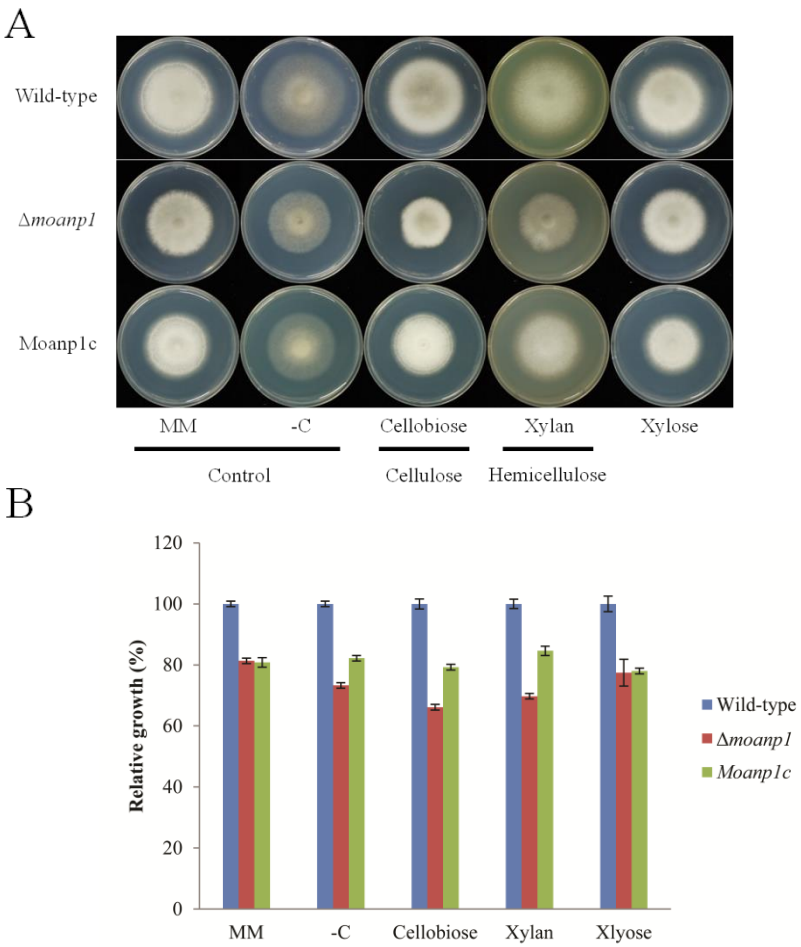


**Figure 10. CWDE utility of Δ*Moanp1* in media**

Mycelia disc were inoculated on mono-carbon source containing starvation media. Growth was measured at 9 dpi. Five component were minimal media which has 1% glucose for nutrient (MMA), Carbon source starvation media (-C), 1% of cellobiose, xylan and xylose respectively contained starvation media (Cellobiose, Xylan and Xlylose). (A) Photographs were taken on the 9 days from inoculation. (B) Growth was measured by relative growth late compared to growth of wild-type.

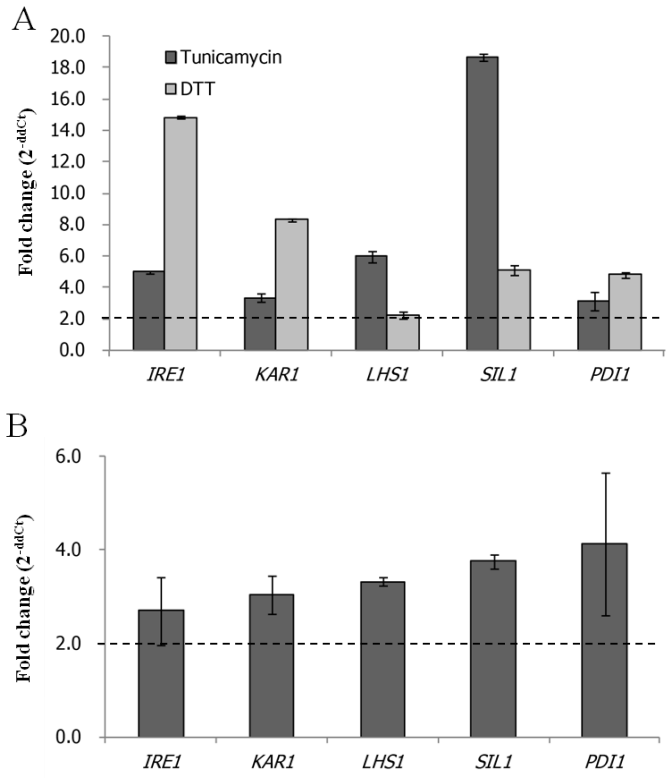


**Figure 11. Expression profiles of UPR pathway genes under ER stress conditions and Δ*Moalg8***

Expression profiling of unfolded protein response (UPR) pathway genes based on the condition of ER stress and Δ*Moalg8* by quantitative real-time PCR. (A) The background samples were cultured from conidial suspension in complete liquid media, 2 days and treated with 10 mM tunicamycin, 60 minutes and 10 ㎍/㎖ DTT, 30 minutes. The result is normalized by the house keeping gene (β-tubulin). Then normalized data were compared with not treated condition. (B) Profiles based on the sample of Δ*Moalg8* and wild-type cultured in the complete liquid media and normalized by β-tubulin gene.

# DISCUSSION

Process of secretion and its products secreted effector proteins interacting with plant are key players in pathogenesis (Kamoun, 2006; Nimchuk *et al.*, 2003). The effector secretion mechanisms of bacterial pathogens have been largely unveiled, but only a little is characterized for eukaryote plant pathogens. Many secretion proteins have signal peptide at N-terminal for translocation into ER, which occurs in classical ER-Golgi-mediated secretion system (Zimmermann *et al.*, 2006). After the translocation, secretion proteins are processed by the post-translational modification. Especially, glycosylation is one of the key processes of protein modification in ER (Roth, 2002).

For the screening of glycosylation genes, bioinformatics tools were applied to collect the candidate and compensate the misjudgment of orthologs. To avoid mismatch of outparalog to orthologs, two respective programs were used to double filter them. In the union, one set was from the mostly matched loci by BLASTP and the other set was loci filtered by Inparanoid 7.0. As a result, 37 homologs were collected in *M. oryzae* function of glycosylation in *S. cerevisiae*. T-DNA insertion mutant library (Choi *et al.*, 2007) was used for focusing on the pathogenesis related genes and 7 T-DNA insertion mutants were selected among the 37 homologs. In order to filter the genes whether the

disruption of genes has an effect on pathogenesis or not, spray inoculation was performed. As a result, disruption of *MoANP1* and *MoALG8* showed reduced pathogenicity.

In this study, we investigated the two glycosylated proteins having an effect on pathogenicity. *MoANP1* and *MoALG8* are highly related to symptom development on rice cultivar. *MoANP1* are also essential for vegetative growth and conidiation. *MoANP1* not only plays the key role in vegetative growth, but also pathogenesis in rice.

MoANP1 is predicted to have an Anp1 domain known as domain of mannosyltransferase grouped in GH62 (Cantarel *et al.*, 2009). It is also predicted to contain one trans-membrane helix and one N-glycosylation site. Function of MoANP1 is related to glycosylation branching in the Golgi apparatus (Chapman and Munro, 1994). Δ*Moanp1* showed the reduction of vegetative growth on complete media, and these result came from cataclysmic change in cell wall. It was demonstrated by growth reduction at cell wall stress agents, calcofluor white (CFW) and congo red (CR) added complete media, relative growth of complete media. CFW and CR are working as inhibitor of 1,3-β-glucan linked to chitin structure in the filamentous fungi (Ram and Klis, 2006). Furthermore 1,3-β-glucan is inner part of mannoprotein layer and outer layer of chitin layer in three layered cell wall classification (Bowman and Free,

2006). This connotes that MoANP1 affected cell wall layer influence the growth defects.

Conidiation was also reduced compared to wild-type and conidiophore was malformed in the colony. While the flaws were observed in developmental stages before the conidial germination, germination and appressoria formation were completed normally in mutant strain. However invasive growth in plant was delayed and hardly burst into the adjacent cells. It also displayed reduction of mycelia growth in mono-carbon source media, related to cell wall structure. Cellobiose and xylan are basic structure of cellulose and hemicellulose respectively which is major component of plant cell wall (McNeil *et al.*, 1984). Invasive hypha is reveal the cell to cell movement and utilize the nutrient from dead cell in late stage of infection (*in planta* condition of 72hpi) Both utilization of nutrient and cell to cell movement are highly related to plant CWDEs like cellulase and xylanase (Wu *et al.*, 2006). Δ*Moanp1* showed the reduction of growth at specific mono-carbon source (cellobiose and xylan) conditions like C starvation condition. Δ*Moanp1* affected the degradation enzymes, as a result the decrease in the activities of plant CWDEs *in planta* condition might be related to reduction of invasive growth.

MoALG8 is composed of eleven transmembrane helixes and one N-glycosylation site. It has glucosyltranferase domain of ALG6/ALG8, grouped

in GT57 (Cantarel *et al.*, 2009), which is known to work in endoplasmic reticulum. Function of this domain involves in the act of adding the terminal glycan complex in early stage of secretion (Stagljar *et al.*, 1994). Δ*Moalg8* showed reduction of virulence. Although the developments before the penetration into plant did not show any defect, invasive growth in plant was captured to one cell. The terminal glycan complex had well identified as quality check point of protein folding and deeply related to unfolded protein response (UPR) pathway (Helenius and Aebi, 2004; Ruddock and Molinari, 2006). The ER stress-related UPR pathway is described as having relationship with glycosylation, attenuation of protein synthesis and retrieving of misfolded proteins to cytosol for degradation (Liu and Kaufman, 2005). This pathway is well known for its conservation of main function, overcoming the malicious effects by accumulating misfolded proteins. (Marciniak and Ron, 2006; Ni and Lee, 2007) The expression profiling of UPR pathway in Δ*Moalg8* showed the similar increasing pattern of ER stress conditions. Thus disruption of *MoALG8* activated the UPR pathway and overloaded to ER systems. Induction of UPR revealed attenuated protein secretion and improper protein process during post-translation modification (Yi *et al.*, 2009). Therefore the disruption of glycosylation could affect secreted protein and this might capture the invasive growth in the one host cells.

Taken together, *MoANP1* is required to produce the cell wall components for structuring the layers and secretes normal acting plant CWDE to cause virulence at the late infection stage. *MoALG8* is related to UPR pathway working as secretory machinery for quality check of misfolded proteins. This gene might be regulatory point of invasive growth in the host cell. The findings and logical implications in this study, may be milestone to unveil glycosylation as a novel mechanism of pathogenesis in *M. oryzae*.

# LITERATURE CITED


Annis, S.L., Goodwin, P.H. (1997) Recent advances in the molecular genetics of plant cell wall-degrading enzymes produced by plant pathogenic fungi. *Eur. J. Plant Pathol.* **103**: 1-14.

Bause, E. (1983) Structural requirements of N-glycosylation of proteins. Studies with proline peptides as conformational probes. *Biochem. J.* **209**: 331-336.

Bendtsen, J.D., Jensen, L.J., Blom, N., Von Heijne, G., Brunak, S. (2004) Feature-based prediction of non-classical and leaderless protein secretion. *Protein engineering, design & selection : PEDS* **17**: 349-356.

Bowman, S.M., Free, S.J. (2006) The structure and synthesis of the fungal cell wall. *Bioessays* **28**: 799-808.

Branza-Nichita, N., Petrescu, A.J., Negroiu, G., Dwek, R.A., Petrescu, S.M. (2000) N-glycosylation processing and glycoprotein folding-lessons from the tyrosinase-related proteins. *Chem. Rev.* **100**: 4697-4712.

Cantarel, B.L., Coutinho, P.M., Rancurel, C., Bernard, T., Lombard, V., Henrissat, B. (2009) The Carbohydrate-Active EnZymes database (CAZy): an expert resource for Glycogenomics. *Nucleic Acids Res* **37**: D233-238.

Carraway, K.L., Hull, S.R. (1989) O-glycosylation pathway for mucin-type glycoproteins. *Bioessays* **10**: 117-121.

Chaffin, W.L., Lopez-Ribot, J.L., Casanova, M., Gozalbo, D., Martinez, J.P. (1998) Cell wall and secreted proteins of Candida albicans: identification, function, and expression. *Microbiol. Mol. Biol. Rev.* **62**: 130-180.

Chapman, R.E., Munro, S. (1994) The functioning of the yeast Golgi apparatus requires an ER protein encoded by ANP1, a member of a new family of genes affecting the secretory pathway. *EMBO J.* **13**: 4896-4907.

Choi, J., Park, J., Jeon, J., Chi, M.H., Goh, J., Yoo, S.Y., Park, J., Jung, K., Kim, H., Park, S.Y., Rho, H.S., Kim, S., Kim, B.R., Han, S.S., Kang, S., Lee, Y.H. (2007) Genome-wide analysis of T-DNA integration into the chromosomes of Magnaporthe oryzae. *Mol. Microbiol.* **66**: 371-382.

Couch, B.C., Fudal, I., Lebrun, M.H., Tharreau, D., Valent, B., van Kim, P., Notteghem, J.L., Kohn, L.M. (2005) Origins of host-specific populations of the blast pathogen Magnaporthe oryzae in crop

domestication with subsequent expansion of pandemic clones on rice and weeds of rice. *Genetics* **170**: 613-630.
Crocker, P.R., Feizi, T. (1996) Carbohydrate recognition systems: functional triads in cell-cell interactions. *Curr. Opin. Struct. Biol.* **6**: 679-691.
Dean, R.A., Talbot, N.J., Ebbole, D.J., Farman, M.L., Mitchell, T.K., Orbach, M.J., Thon, M., Kulkarni, R., Xu, J.R., Pan, H.Q., Read, N.D., Lee, Y.H., Carbone, I., Brown, D., Oh, Y.Y., Donofrio, N., Jeong, J.S., Soanes, D.M., Djonovic, S., Kolomiets, E., Rehmeyer, C., Li, W.X., Harding, M., Kim, S., Lebrun, M.H., Bohnert, H., Coughlan, S., Butler, J., Calvo, S., Ma, L.J., Nicol, R., Purcell, S., Nusbaum, C., Galagan, J.E., Birren, B.W. (2005) The genome sequence of the rice blast fungus *Magnaporthe grisea*. *Nature* **434**: 980-986.
Deshpande, N., Wilkins, M.R., Packer, N., Nevalainen, H. (2008) Protein glycosylation pathways in filamentous fungi. *Glycobiology* **18**: 626-637.
Ebbole, D.J. (2007) Magnaporthe as a model for understanding host-pathogen interactions. *Annu Rev Phytopathol* **45**: 437-456.
Geysens, S., Whyteside, G., Archer, D.B. (2009) Genomics of protein folding in the endoplasmic reticulum, secretion stress and glycosylation in the aspergilli. *Fungal Genet. Biol.* **46**: S121-S140.
Gilbert, M.J., Thornton, C.R., Wakley, G.E., Talbot, N.J. (2006) A P-type ATPase required for rice blast disease and induction of host resistance. *Nature* **440**: 535-539.
Hampton, R.Y. (2000) ER stress response: getting the UPR hand on misfolded proteins. *Current biology : CB* **10**: R518-521.
Helenius, A., Aebi, M. (2004) Roles of N-linked glycans in the endoplasmic reticulum. *Annu. Rev. Biochem.* **73**: 1019-1049.
Herscovics, A. (1999) Processing glycosidases of Saccharomyces cerevisiae. *Biochim. Biophys. Acta* **1426**: 275-285.
Howard, R.J., Ferrari, M.A., Roach, D.H., Money, N.P. (1991) Penetration of hard substrates by a fungus employing enormous turgor pressures. *Proceedings of the National Academy of Sciences of the United States of America* **88**: 11281-11284.
Kamoun, S. (2006) A catalogue of the effector secretome of plant pathogenic oomycetes. *Annu Rev Phytopathol* **44**: 41-60.
Kankanala, P., Czymmek, K., Valent, B. (2007) Roles for rice membrane dynamics and plasmodesmata during biotrophic invasion by the blast fungus. *Plant Cell* **19**: 706-724.
Kasuya, T., Nakajima, H., Kitamoto, K. (1999) Cloning and characterization of the bipA gene encoding ER chaperone BiP from Aspergillus oryzae. *J Biosci Bioeng* **88**: 472-478.

Khang, C.H., Berruyer, R., Giraldo, M.C., Kankanala, P., Park, S.Y., Czymmek, K., Kang, S., Valent, B. (2010) Translocation of Magnaporthe oryzae effectors into rice cells and their subsequent cell-to-cell movement. *Plant Cell* **22**: 1388-1403.

Kim, S., Ahn, I.P., Rho, H.S., Lee, Y.H. (2005) MHP1, a Magnaporthe grisea hydrophobin gene, is required for fungal development and plant colonization. *Mol. Microbiol.* **57**: 1224-1237.

Lau, G.W., Hamer, J.E. (1998) Acropetal: a genetic locus required for conidiophore architecture and pathogenicity in the rice blast fungus. *Fungal Genet. Biol.* **24**: 228-239.

Lee, J., Park, J.S., Moon, J.Y., Kim, K.Y., Moon, H.M. (2003) The influence of glycosylation on secretion, stability, and immunogenicity of recombinant HBV pre-S antigen synthesized in Saccharomyces cerevisiae. *Biochem. Biophys. Res. Commun.* **303**: 427-432.

Lippincott-Schwartz, J., Roberts, T.H., Hirschberg, K. (2000) Secretory protein trafficking and organelle dynamics in living cells. *Annu. Rev. Cell Dev. Biol.* **16**: 557-589.

Lussier, M., Sdicu, A.M., Bussereau, F., Jacquet, M., Bussey, H. (1997) The Ktr1p, Ktr3p, and Kre2p/Mnt1p mannosyltransferases participate in the elaboration of yeast O- and N-linked carbohydrate chains. *J. Biol. Chem.* **272**: 15527-15531.

Maras, M., De Bruyn, A., Vervecken, W., Uusitalo, J., Penttila, M., Busson, R., Herdewijn, P., Contreras, R. (1999) In vivo synthesis of complex N-glycans by expression of human N-acetylglucosaminyltransferase I in the filamentous fungus Trichoderma reesei. *FEBS Lett.* **452**: 365-370.

Marciniak, S.J., Ron, D. (2006) Endoplasmic reticulum stress signaling in disease. *Physiol. Rev.* **86**: 1133-1149.

Mauri, C., Bosma, A. (2012) Immune regulatory function of B cells. *Annu. Rev. Immunol.* **30**: 221-241.

McNeil, M., Darvill, A.G., Fry, S.C., Albersheim, P. (1984) Structure and function of the primary cell walls of plants. *Annu. Rev. Biochem.* **53**: 625-663.

Mosquera, G., Giraldo, M.C., Khang, C.H., Coughlan, S., Valent, B. (2009) Interaction transcriptome analysis identifies Magnaporthe oryzae BAS1-4 as Biotrophy-associated secreted proteins in rice blast disease. *Plant Cell* **21**: 1273-1290.

Ni, M., Lee, A.S. (2007) ER chaperones in mammalian development and human diseases. *FEBS Lett.* **581**: 3641-3651.

Nimchuk, Z., Eulgem, T., Holt, B.F., 3rd, Dangl, J.L. (2003) Recognition and response in the plant immune system. *Annu. Rev. Genet.* **37**: 579-609.

O'Brien, K.P., Remm, M., Sonnhammer, E.L. (2005) Inparanoid: a comprehensive database of eukaryotic orthologs. *Nucleic Acids Res* **33**: D476-480.

Ochman, H., Gerber, A.S., Hartl, D.L. (1988) Genetic applications of an inverse polymerase chain reaction. *Genetics* **120**: 621-623.

Ostlund, G., Schmitt, T., Forslund, K., Kostler, T., Messina, D.N., Roopra, S., Frings, O., Sonnhammer, E.L. (2010) InParanoid 7: new algorithms and tools for eukaryotic orthology analysis. *Nucleic Acids Res* **38**: D196-203.

Ou, S.H. (1985) *Rice diseases.* Surrey: Commonwealth Mycological Institute.

Rafiqi, M., Ellis, J.G., Ludowici, V.A., Hardham, A.R., Dodds, P.N. (2012) Challenges and progress towards understanding the role of effectors in plant-fungal interactions. *Curr. Opin. Plant Biol.* **15**: 477-482.

Ram, A.F., Klis, F.M. (2006) Identification of fungal cell wall mutants using susceptibility assays based on Calcofluor white and Congo red. *Nat Protoc* **1**: 2253-2256.

Roth, J. (2002) Protein N-glycosylation along the secretory pathway: relationship to organelle topography and function, protein quality control, and cell interactions. *Chem. Rev.* **102**: 285-303.

Ruddock, L.W., Molinari, M. (2006) N-glycan processing in ER quality control. *J. Cell Sci.* **119**: 4373-4380.

Song, W., Dou, X., Qi, Z., Wang, Q., Zhang, X., Zhang, H., Guo, M., Dong, S., Zhang, Z., Wang, P., Zheng, X. (2010) R-SNARE homolog MoSec22 is required for conidiogenesis, cell wall integrity, and pathogenesis of Magnaporthe oryzae. *Plos One* **5**: e13193.

Stagljar, I., te Heesen, S., Aebi, M. (1994) New phenotype of mutations deficient in glucosylation of the lipid-linked oligosaccharide: cloning of the ALG8 locus. *Proc. Natl. Acad. Sci. U. S. A.* **91**: 5977-5981.

Stergiopoulos, I., de Wit, P.J. (2009) Fungal effector proteins. *Annual review of phytopathology* **47**: 233-263.

Stukenbrock, E.H., McDonald, B.A. (2009) Population genetics of fungal and oomycete effectors involved in gene-for-gene interactions. *Mol. Plant. Microbe Interact.* **22**: 371-380.

Talbot, N.J. (2003) On the trail of a cereal killer: Exploring the biology of Magnaporthe grisea. *Annu. Rev. Microbiol.* **57**: 177-202.

Talbot, N.J., Ebbole, D.J., Hamer, J.E. (1993) Identification and characterization of MPG1, a gene involved in pathogenicity from the rice blast fungus Magnaporthe grisea. *Plant Cell* **5**: 1575-1590.

Valent, B. (1990) Rice blast as a model system for plant pathology. *Phytopathology* **80**: 33-36.

Valent, B., Farrall, L., Chumley, F.G. (1991) *Magnaporthe grisea* genes for pathogenicity and virulence identified through a series of backcrosses. *Genetics* **127**: 87-101.

van de Veerdonk, F.L., Netea, M.G., Jansen, T.J., Jacobs, L., Verschueren, I., van der Meer, J.W., Kullberg, B.J. (2008) Redundant role of TLR9 for anti-Candida host defense. *Immunobiology* **213**: 613-620.

Wu, S.C., Halley, J.E., Luttig, C., Fernekes, L.M., Gutierrez-Sanchez, G., Darvill, A.G., Albersheim, P. (2006) Identification of an endo-beta-1,4-D-xylanase from Magnaporthe grisea by gene knockout analysis, purification, and heterologous expression. *Applied and environmental microbiology* **72**: 986-993.

Yi, M., Chi, M.H., Khang, C.H., Park, S.Y., Kang, S., Valent, B., Lee, Y.H. (2009) The ER chaperone LHS1 is involved in asexual development and rice infection by the blast fungus Magnaporthe oryzae. *Plant Cell* **21**: 681-695.

Yu, J.H., Hamari, Z., Han, K.H., Seo, J.A., Reyes-Dominguez, Y., Scazzocchio, C. (2004) Double-joint PCR: a PCR-based molecular tool for gene manipulations in filamentous fungi. *Fungal Genet. Biol.* **41**: 973-981.

Yun, S.H. (1998) Molecular genetics and manipulation of pathogenicity and mating determinants in Mycoshpaerella zeae-maydis and Cochlobolus heterostrophus. Ph.D. thesis. Cornell University, Ithaca, N.Y.

Zadoks, J.C., Chang, T.T., Konzak, C.F. (1974) Decimal Code for Growth Stages of Cereals. *Weed Res.* **14**: 415-421.

Zimmermann, R., Muller, L., Wullich, B. (2006) Protein transport into the endoplasmic reticulum: mechanisms and pathologies. *Trends Mol Med* **12**: 567-573.

# 벼 도열병균의 병 발생과정에 관여하는 당질화 관련 유전자들의 특성 규명

전 종 범

## 초 록

벼 도열병균은 전세계적으로 벼를 재배하는 지역에서 심각한 피해를 주는 식물병원균이다. 이 도열병은 식물과 병원체간의 관계를 이해하는데 모델시스템이다. 도열병균의 병 발생과정을 완성하기 위해 소포체에서의 분비 메커니즘은 중요하다. 분비 메커니즘 중에 하나인 당질화 과정은 단백질 안정화와 Quality control 에 관련된 역할을 한다고 알려져 있다. 이 당화과정은 식물병원균에서는 아직 연구된 바가 거의 없다. 당질화 과정 유전자를 선별하기 위해 먼저 상호 BLASTP 연구를 통하여 효모의 유전자에 대응하는 37 개의 도열병균 당질화 유전자를 선별하였다. T-DNA 삽입 유전체 library 를 이용하여 병원성이 야생형에 비해 줄은 2 개의 유전자를 찾았다. 이 두 유전자는 각각 *MoANP1* 와

*MoALG8* 의 유전자 근처에 삽입되어 있으며, N-당질화 과정에서 당기를 붙이는 기능을 하고 있다. 이 두 유전자의 기능을 분석하기 위해 유전자 치환방법을 이용하여 유전자 삭제 변이체를 제작하였다. 이 두 유전자의 삭제 변이체는 잎에서의 병진전과 침입균사의 병 발생이 지연되었다. 그리고 여러 표현형질로써 Δ*Moanp1* 의 경우 야생형에 비해 60%정도의 분생 포자를 형성하였으며, 세포벽 결함을 확인할 수 있는 Congo red 배지에서 균사생장에 영향을 보였다. 또한 세포벽 분해효소의 활성이 저하되었다. Δ*Moalg8* 의 경우 병 발생을 제외한 다른 병 발달 과정에서 야생형과 차이를 보이지 않았다. 그러나 당질화 과정 억제제인 tunicamycin 을 처리하였을 때 UPR 회로와 관련된 6 개의 유전자들의 발현이 증가하였고, 또한 Δ*Moalg8* 에서의 6 개 유전자 발현 역시 비슷한 양상을 보였다. 본 연구의 결과를 종합하였을 때 당화과정에 관련된 두 유전자는 병원성 과정에 있어 당질화 과정 유전자가 관여함을 보여주고 있다.

주요어 : 당질화 과정, 벼 도열병균, 병원성, 분비 메커니즘

학번: 2011-23535